

# Effects of shrub encroachment on vertical changes in soil organic carbon in Mongolian grasslands: using a multi-biomarker approach

Luhong Zhou  · He Li · Haihua Shen · Yunping Xu · Yinghui Wang · Aijun Xing · Yankun Zhu · Shangzhe Zhou · Jingyun Fang

Received: 11 January 2018 / Accepted: 20 July 2018 / Published online: 26 July 2018  
© Springer Nature Switzerland AG 2018

## Abstract

**Aims** In recent decades, ecologists have investigated the effects of shrub encroachment on regional carbon cycling in semi-arid and arid regions. Although differences in carbon sequestration and stocks have been recognized in different soil layers, the vertical changes in soil organic carbon (SOC) at the molecular level following shrub encroachment remain unexplored. In this study, we used biomarkers to assess the impacts of shrub encroachment on SOC composition.

**Methods** We collected soil samples along the 1-m profile within shrub patches and grassy matrix in three typical shrub-encroached grassland (SEG) sites in Inner Mongolia, and quantified the vertical distribution of the biomarkers, including free lipids, bound lipids and lignin-derived phenols.

**Results** The principal component analysis (PCA) of the biomarker data showed that samples in the grassy matrix had strong positive loadings along the first two components (PCs); in contrast, samples in the upper 50 cm of the shrub patches had negative loadings along the first component (PC1) as well as a narrower range. The acid to aldehyde ratios of the vanillyl and syringyl type monomers increased simultaneously along the 1-m profile in the grassy matrix; however, this trend was not observed in the shrub patches. In addition, the vanillyls to syringyls to cinnamyls ratio was approximately 3:2:1 in the shrub patches and 3:2:1 or 2:2:1 in the grassy matrix.

**Conclusions** Shrub encroachment altered the vertical patterns in SOC composition, especially in the upper 50 cm, as well as the oxidation status of lignin-derived phenols along the entire 1-m profile. Further, shrub encroachment influenced the soil carbon composition under the shrub canopy as well as in the grassy matrix due to the sprawling canopies and the horizontal extension of the root systems of the encroaching shrubs. These results provided new insights into the vertical patterns of SOC changes after shrub encroachment at the molecular level and have important implications for understanding the mechanisms of soil carbon dynamics with changes in vegetation structure and composition.

---

Responsible Editor: Ingrid Koegel-Knabner.

L. Zhou · H. Li · H. Shen · A. Xing · Y. Zhu · J. Fang  
State Key Laboratory of Vegetation and Environmental Change,  
Institute of Botany, Chinese Academy of Sciences,  
Beijing 100093, China

L. Zhou · H. Shen · A. Xing · Y. Zhu · J. Fang  
University of Chinese Academy of Sciences, Beijing 100049,  
China

Y. Xu  
Shanghai Engineering Research Center of Hadal Science and  
Technology, College of Marine Sciences, Shanghai Ocean  
University, Shanghai 201306, China

Y. Wang · S. Zhou · J. Fang (✉)  
College of Urban and Environmental Sciences, and Key  
Laboratory of Earth Surface Processes of the Ministry of  
Education, Peking University, Beijing 100871, China  
e-mail: jyfang@urban.pku.edu.cn  
e-mail: fangjingyun@ibcas.ac.cn

**Keywords** Carbon cycling · Lignin · Plant-soil feedback · Principal component analysis · Shrub encroachment · Soil process

## Introduction

Over the past 150 years, a phenomenon in which the cover or density of natural shrubs increases in grassland and savanna ecosystems, commonly defined as “shrub encroachment”, has been reported in arid and semi-arid regions (Van Auken 2009; Eldridge et al. 2011; Chen et al. 2015). Shrub encroachment usually leads to a landscape characterized by shrub patches embedded in the grassland matrix, and affects the plant species richness, production, hydrological properties and soil nutrients of the grasslands (Eldridge et al. 2011; Peng et al. 2013; Li et al. 2016). Of particular importance are the effects of shrub encroachment on the cycling of soil organic carbon (SOC), which is the largest pool of organic carbon (OC) in terrestrial ecosystems (Schmidt et al. 2011). However, there is no consensus regarding changes in SOC stock after shrub encroachment, which has been shown to increase (Maestre et al. 2009; Blaser et al. 2014), remain stable (Hughes et al. 2006), or decrease (Jackson et al. 2002; Oelofse et al. 2016). These inconsistencies can be ascribed to differences in the soil characteristics, historical land-use patterns and sampling depths (Zhou et al. 2017a). Given that topsoil is the most sensitive to environmental changes, previous studies that evaluated the impacts of shrub encroachment have focused on the upper 20–30 cm of soils (Maestre et al. 2009; Saixiyala et al. 2017). However, there is increasing evidence that deeper soils (i.e., below 50 cm) have a strong potential ability to sequester carbon; therefore, a comprehensive investigation of the vertical changes of SOC following shrub encroachment is needed (Zhou et al. 2017b).

Due to vertical changes in substrate quality and microbial activity with soil depth, the carbon dynamics and biological processes are quite different between topsoil and deeper soil (Salomé et al. 2010; Rumpel and Kögel-Knabner 2011). Previous studies have demonstrated that the quality and quantity of aboveground litter contribute to the accumulation of SOC in the top layer (Fillye et al. 2008; Tamura and Tharayil 2014); in contrast, roots and rhizodeposition are the main carbon sources in the deeper soil layers (Jobbágy and Jackson 2000; Zhou et al. 2017b). The chemistry and quantity of above-

and belowground plant inputs are commonly different, and these inputs can be traced by molecular-level analyses (Crow et al. 2009; Angst et al. 2016). Therefore, characterizing the vertical distribution patterns of SOC changes following shrub encroachment at the molecular level can help model the carbon dynamics in deep soil. Additionally, this understanding is crucial for understanding how changes in vegetation composition can affect the SOC pool.

Organic matter (OM) biomarkers have been used successfully to assess the source and degradation of SOC (Kögel-Knabner 2002; Feng and Simpson 2011). For example, dichloromethane-methanol-extractable  $C_{16}$ - $C_{30}$  *n*-alkanoic acids (FAs) and long-chain ( $>C_{20}$ ) *n*-alkanes and *n*-alkanols are predominantly derived from vascular plants, while the short-chain ( $<C_{20}$ ) alkanols indicate a microbial origin in an Inner Mongolian grassland (Zhou et al. 2017a). Although the individual composition varies according to the plant species, cutin and suberin monomers in bound lipids are typical biomarkers of underground and belowground inputs, respectively (Bull et al. 2000; Nierop et al. 2003; Crow et al. 2009; Feng et al. 2010). In addition, lignin, which consists of a polymeric network of phenols (e.g., cinnamyls, syringyls and vanillyls), is specific to vascular plants. For example, the cinnamyls/vanillyls (C/V) ratio indicates non-woody tissues and grasses because of the absence of C-type lignin phenols in woody tissues; the syringyls/vanillyls (S/V) ratio indicates angiosperm-derived OM because gymnosperms (e.g., conifers) do not contain S-type lignin phenols (Hedges and Mann 1979). In addition, the ratios of acids to aldehydes in lignin phenols (i.e., Ad/Al) are related to the degradation status of soil organic matter (SOM) (Feng and Simpson 2011). Together, these biomarkers can provide detailed information about vegetation (Angst et al. 2016). In grasslands and forests, biomarker contents change with soil depth (Rumpel et al. 2004; Feng and Simpson 2007; Angst et al. 2016), suggesting the possibility of understanding the vertical distribution of SOC at the molecular level. Biomarker analysis has been applied to examine the SOM responses to climate change (Feng et al. 2010; Pisani et al. 2015) and land use change (Zhao et al. 2014; Armas-Herrera et al. 2016) in grasslands (Otto and Simpson 2005, 2006; Feng and Simpson 2007), forests (Feng et al. 2010; Angst et al. 2016) and shrublands (Cai et al. 2017). However, very few studies have examined the vertical distribution of SOC composition in shrub-encroached grasslands

(SEGs), where the vegetation and chemical compositions of SOM are markedly different from those in forests and grasslands (Kögel-Knabner 2002; Feng and Simpson 2007).

Shrub encroachment is prevalent in the grasslands of Inner Mongolia. Compared to herbaceous plants, shrubs provide more aboveground litter and deep roots in soil at a depth of 1.2 m (Knapp et al. 2008; Rumpel and Kögel-Knabner 2011; Zhou et al. 2017b). In this study, we assessed the compositional changes in SOM in entire 1-m soil profiles following shrub encroachment in Inner Mongolian grasslands. Our objectives were to (1) estimate the vertical distribution of plant-derived carbon components, including free lipids, bound lipids and lignin phenols in the shrub patches and the grassy matrix; and (2) determine the underlying mechanisms by which shrub encroachment induced changes in SOC.

## Materials and methods

### Study sites and soil sampling

We selected three study sites in nearby SEGs in Inner Mongolia. These sites included the typical shrub species *Caragana microphylla* and *Amygdalus pedunculata*. This grassland ecosystem is characterized by a temperate continental monsoon climate. The soils are predominantly Kastanozems (IUSS Working Group WRB 2015), and the 1-m profile had A<sub>h</sub> (20–40 cm), B<sub>k</sub> (25–45 cm), and C horizons (National soil survey office 1994). Table 1 lists the climate and vegetation characteristics of the study sites. The root depths of the dominant shrubs *C. microphylla* and *A. pedunculata* in our study areas could reach 1.8–2.2 m and 1.7 m, respectively (Niu et al. 2013; Zhang et al. 2013; Wang et al. 2017).

At each site, soil samples were taken from three uniform shrub canopies (with diameters greater than 1 m) and from the grassy matrix in September 2013. Within each shrub patch, three cores of soil were collected using a stainless-steel corer, and then mixed into one soil sample. Moreover, three cores located at least 3 m from the nearest shrub were also collected from each site (Fig. 1). Soil samples were collected at fixed depths (0–10, 10–20, 20–30, 30–50, 50–70 and 70–100 cm), an approach that has been widely used to estimate SOC vertical dynamics along the soil profile (Toriyama et al. 2011; Blaser et al. 2014; Li 2015; Zhou

et al. 2017b). All the soil samples were stored at –20 °C until analysis.

### Soil pretreatment and elemental analyses

Grasses have a dense, fibrous root system in the upper 20–30 cm of the soil profiles, while shrubs have a greater root depth (Briske 2017). Correspondingly, shrub encroachment had no significant effects on the upper 30 cm based on our previous studies at the regional scale (Li 2015). In addition, the A<sub>h</sub> horizon in our study areas was approximately 20–40 cm. Taking these results into consideration, we combined the upper 30 cm of the soil samples as topsoil to analyze the vertical distribution of SOC. All samples were air-dried, and then sieved through a 2-mm sieve. The plant roots were carefully removed from the soil samples using tweezers, and the soil samples were ground thoroughly using a grinder. The soil total carbon (STC) and soil total nitrogen (STN) contents were measured using an elementary analyzer (Vario EL III, Elementar, Germany). The soil inorganic carbon (SIC) content was quantified using a carbonate content analyzer (Eijkelkamp 08.53, Netherlands). Finally, the SOC was calculated by subtracting the SIC from the STC.

### Chemical extractions and GC/MS analysis

Sequential chemical extractions, including solvent extraction, base hydrolysis and copper (II) oxide (CuO) oxidation, were conducted to isolate the free lipids, bound lipids and lignin-derived phenols, respectively (a flowchart is shown in Fig. 2; Feng et al. 2010; Zhao et al. 2014; Zhou et al. 2017a). Briefly, soil samples (~6 g from 0 to 30 and 30–50 cm or ~9 g from 50 to 70 and 70–100 cm) were extracted using 15 mL of chromatography-grade dichloromethane (DCM): methanol (MeOH) (1:1; v: v) by ultrasonication for 15 min (Zhao et al. 2014; Zhou et al. 2017a). The extracts were centrifuged at 3500 rpm for 10 min, and the supernatants were transferred into 150-mL pre-combusted flasks. The extraction was repeated three times for each sample. The combined solvent extracts were filtered using glass fiber columns and concentrated by rotary evaporation. Approximately 3 g air-dried residues from the solvent extraction were heated at 100 °C for 3 h with 15 mL of 1 mol/L KOH/MeOH. Next, the suspension was acidified to a pH of 1 with 6 mol/L HCl. The bound lipids were recovered by liquid-liquid extraction with 20 mL

**Table 1** Climate and vegetation characteristics in the study sites. MAT, mean annual temperature; MAP, mean annual precipitation

Site	Latitude (°N)	Longitude (°E)	MAT (°C)	MAP (mm)	Shrub cover (%)	Dominant shrub plants	Dominant herbaceous plants
1	42.33	114.30	3.9	287	7.3	<i>Caragana microphylla</i>	<i>Stipa krylovii</i> , <i>Allium ramosum</i> , <i>Melilotoides ruthenica</i>
2	42.57	112.44	4.4	211	16.8	<i>Amygdalus pedunculata</i> , <i>C. stenophylla</i> , <i>C. pygmaea</i> , <i>C. microphylla</i>	<i>Cleistogenes squarrosa</i> , <i>Stipa klemenzii</i> , <i>Agropyron mongolicum</i>
3	42.57	112.43	4.9	213	12.5	<i>A. pedunculata</i> , <i>C. stenophylla</i> , <i>C. pygmaea</i> , <i>C. microphylla</i>	<i>C. squarrosa</i> , <i>Cleistogenes songorica</i> , <i>A. mongolicum</i>

<sup>a</sup> Site 1 is located in the Xianghuang Banner; Sites 2 and 3 are located in the Sonid Right Banner

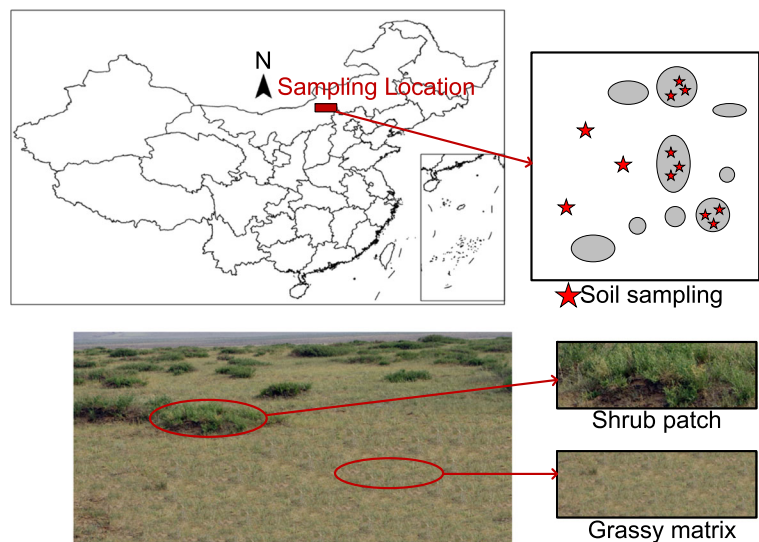
ethyl acetate, and then concentrated by rotary evaporation (Zhao et al. 2014; Zhou et al. 2017a). The product was methylated at 70 °C with 1 mL of 14% BF<sub>3</sub>: MeOH for 90 min, and the bound lipids were obtained by liquid-liquid extraction with 2 mL hexane. For lignin analyses, the air-dried residues after solvent extraction were mixed with 15 mL of 2 mol/L NaOH, 1 g of CuO and 100 mg of ammonium iron (II) sulphate hexahydrate. After the oxygen was exhausted using high-pure N<sub>2</sub> gas, the mixtures were heated at 170 °C for 2.5 h. The supernatant was then acidified to a pH of 1 with 6 mol/L HCl. The extracts were kept in the dark at room temperature for 1 h, because cinnamic acids are unstable and easy to decompose under light. Then, the lignin-derived phenols were recovered by liquid-liquid

extraction with 20 mL ethyl acetate (three times). All biomarkers were identified using an Agilent 7890A gas chromatograph coupled to an Agilent 5973 N quadrupole mass selective detector (GC-MS) and quantified using a flame ionization detector (FID) coupled to the Agilent 7890A instrument (GC-FID). Details of the qualitative and quantitative analyses for all biomarkers were provided by Zhou et al. (2017a). All biomarkers were standardized to mg/g OC.

Establishment of the specific biomarkers and parameters based on the plant characteristics

In our previous paper, we identified biomarker characteristics of the common plants in our study area (Zhou

**Fig. 1** Study location, soil sampling and photos of shrub-encroached grasslands (SEGs)



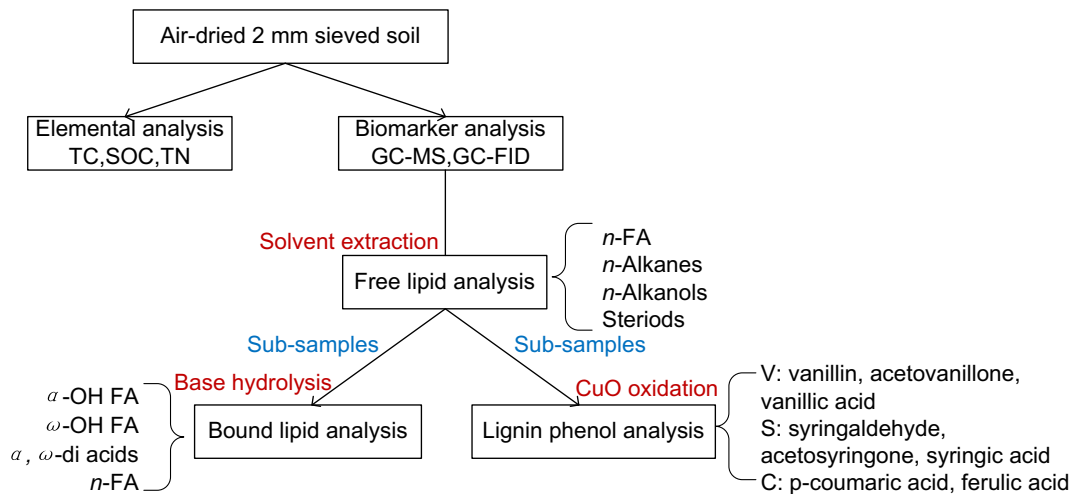


**Fig. 2** Flow chart of elemental analysis and molecular biomarker analysis for soil samples. FA = alkanolic acids

et al. 2017a). Briefly, for free lipids, the leaves were dominated by  $C_{16}$  or  $C_{18}$  *n*-FAs,  $C_{28}$  or  $C_{30}$  *n*-alkanols and  $C_{29}$ – $C_{33}$  *n*-alkanes, while long-chain ( $>C_{20}$ ) *n*-FAs and  $C_{27}$  *n*-alkane were mainly identified in the roots. In addition, *n*-alkanes displayed the maximum abundance at  $C_{29}$  in shrub leaves, but at  $C_{31}$  or  $C_{33}$  in herb leaves. Consistent with previous studies, the short-chain  $\alpha,\omega$ -alkanedioic acids (DAs) and  $\omega$ -hydroxyalkanoic acids (OH FAs) in bound lipids were predominantly identified in leaves, while the long-chain DAs and  $\omega$ -OH FAs were mainly detected in roots (Feng et al. 2010; Zhao et al. 2014; Zhou et al. 2017a). Furthermore, the  $P_{\text{rml}}$  ratio (assessed by the short-chain to the long-chain ratios of *n*-FAs) of leaves were more than five-fold greater than those of the roots. Similarly, the  $C/V$  and  $S/V$  ratios in the leaves (0.30–3.10 and 0.66–3.38) were higher than those in the roots (0.19–2.35 and 0.29–2.26). In contrast, the suberin to cutin ratios in the roots were 5–40 times greater than those in the leaves (Zhou et al. 2017a).

Similarly, the compounds of interest in this present study were categorized based on their structural origin. The free lipids included  $C_{16}$ – $C_{32}$  *n*-FAs,  $C_{22}$ – $C_{30}$  *n*-alkanols,  $C_{27}$ – $C_{31}$  *n*-alkanes and ergosterol. The bound lipids were grouped into  $C_{14}$ – $C_{30}$  bound *n*-FAs,  $C_{16}$ – $C_{24}$  DAs,  $C_{16}$ – $C_{22}$   $\omega$ -OH FAs and  $C_{22}$ – $C_{24}$   $\alpha$ -OH FAs. Among these lipids, the  $C_{16}$  and  $C_{18}$  *n*-FAs,  $C_{28}$  and  $C_{30}$  *n*-alkanols and  $C_{29}$ – $C_{33}$  *n*-alkanes were specific biomarkers for leaves, while the long-chain ( $>C_{20}$ ) *n*-FAs and  $C_{27}$  *n*-alkane were specific biomarkers for roots. In addition,  $C_{29}$  *n*-alkane was a specific indicator of shrub leaves, while  $C_{31}$  *n*-alkane was a specific indicator of herb leaves. Moreover, the predominant

$C_{16}$  and  $C_{18}$   $\omega$ -OH FAs with mid-chain hydroxy or epoxy groups are defined as cutin biomarkers,  $C_{16}$ ,  $C_{18}$   $\omega$ -OH FAs and DAs are biomarkers in both cutin and suberin ( $\Sigma\text{CS}$ ), while long-chain  $\alpha,\omega$ -DAs and  $\omega$ -OH FAs are defined as suberin biomarkers in the present study according to the biomarker characteristics of the local plants (Zhou et al. 2017a). In addition to the  $P_{\text{rml}}$  ratio, the suberin to cutin ratio was also calculated by  $(\text{suberin} + \Sigma\text{CS}) / (\text{cutin} + \Sigma\text{CS})$  to evaluate the relative contribution of aboveground or belowground inputs to the soil. Moreover, the ratios of  $C/V$  and  $S/V$  were calculated as indicators to assess the origins of lignin (Angst et al. 2016; Zhou et al. 2017a). In addition, the ratios of  $\omega\text{-}C_{16}/\Sigma C_{16}$  (sum of  $C_{16}$   $\omega$ -OH FA and DA), syringic acid/syringaldehyde ( $(\text{Ad}/\text{Al})_s$ ) and vanillic acid/vanillin ( $(\text{Ad}/\text{Al})_v$ ) were calculated to assess the degradation of cutin, suberin and lignin (Otto and Simpson 2005, 2006).

#### Statistical analysis

Statistical analyses were conducted using the R 3.3.1 platform (R Foundation for Statistical Computing, Vienna, AT). One-way ANOVA testing was conducted to compare the differences between variables among soils from different depths and to examine the differences between variables in the shrub patch and the grassy matrix from within the same layer. The relative contributions of free lipids, bound lipids and lignin-derived phenols were calculated as their respective contributions to the sum of these three biomarkers (Feng and Simpson 2007). The SOC content, major biomarker



groups and degradation parameters were Z-score normalized and entered into the principal component analysis (PCA) to assess the vertical distribution patterns in SOC composition using the package “vegan”. Similarly, eight lignin compounds were entered into the PCA to evaluate the patterns of lignin.

## Results

### Vertical distribution of the specific biomarkers and parameters in the shrub patches and the grassy matrix

In both the grassy matrix and the shrub patches, the dominant compounds of the solvent extracts from each interest group were  $C_{18}$  *n*-FA,  $C_{28}$  *n*-alkanol and  $C_{31}$  *n*-alkane (Fig. 3). The contents of dominant  $C_{18}$  *n*-FAs (0.39–0.90 mg/g OC),  $C_{28}$  *n*-alkanols (0.17–0.24 mg/g OC) and  $C_{31}$  *n*-alkanes (0.08–0.10 mg/g OC) increased slightly with depth in the grassy matrix; however, in the shrub patches, these three compounds generally decreased downwards, ranging from 0.59 to 0.72, 0.23 to 0.36 and 0.10 to 0.23 mg/g OC, respectively (Fig. 3). In addition, the  $P_{\text{tml}}$  and  $C_{27}/C_{31}$  *n*-alkane ratios generally increased with depth in both the grassy matrix (1.08–1.35 and 0.39–1.15, respectively) and the shrub patches (0.98–1.60 and 0.22–0.62, respectively) (Table 2).

Similar to the solvent extracts, the contents of dominant  $C_{18}$  bound *n*-FA (0.75–5.21 mg/g OC),  $C_{16}$  DAs (0.24–1.47 mg/g OC),  $C_{20}$   $\omega$ -OH FAs (0.27–1.17 mg/g OC) and  $C_{22}$   $\alpha$ -OH FAs (0.00–0.11 mg/g OC) increased with soil depth in the grassy matrix (Fig. 3). In shrub patches, these four components decreased downwards in the upper 50 cm and then increased between 50 and 100 cm, ranging from 0.78 to 2.26 mg/g OC, 0.20 to 0.60 mg/g OC, 0.30 to 0.71 mg/g OC and 0.01 to 0.04 mg/g OC, respectively.

The S/V and C/V ratios decreased in the grassy matrix, ranging from 0.73 to 0.76 and 0.39 to 0.55; in contrast, these ratios varied from 0.72 to 0.80 and from 0.34 to 0.43 in the shrub patches, respectively (Table 2). The  $(\text{Ad}/\text{Al})_s$  and  $(\text{Ad}/\text{Al})_v$  ratios generally increased throughout the entire grassy matrix profiles (0.62–0.74 and 0.71–0.90, respectively), but did not show a clear trend with depth in the shrub patches (0.63–0.68 and 0.80–0.85, respectively).

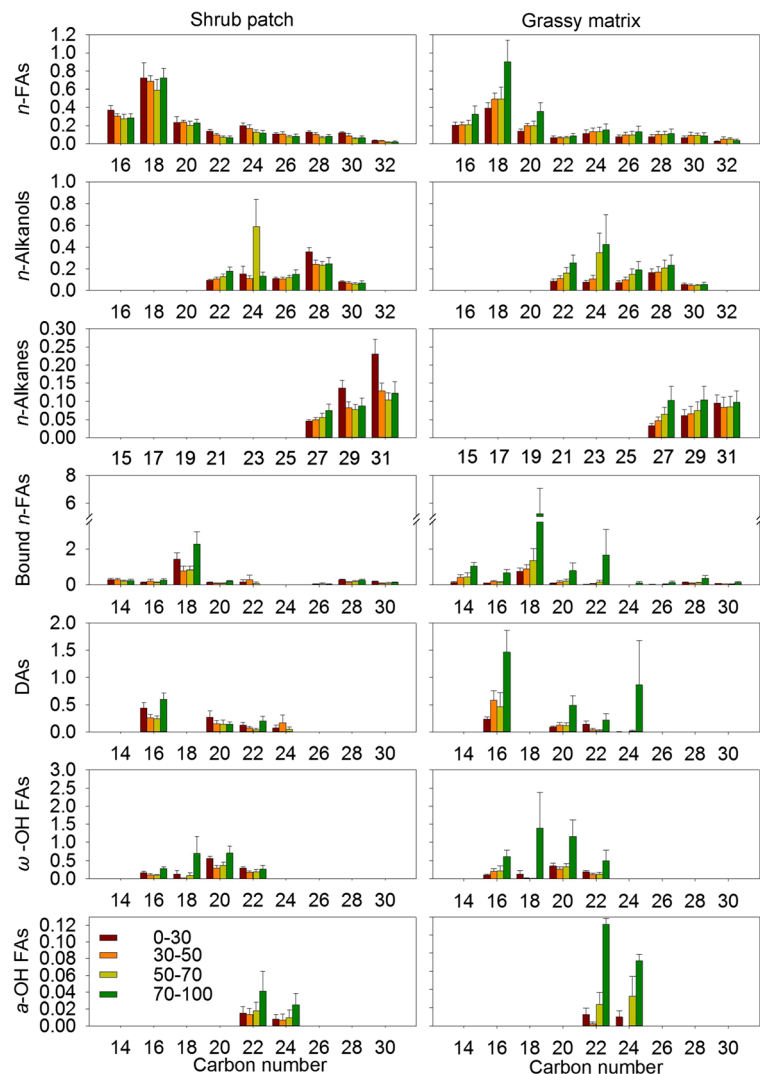
### Vertical distribution of biomarker groups in the shrub patches and the grassy matrix

The vertical distribution differed between the grassy matrix and the shrub patch. The total concentrations of *n*-FAs, *n*-alkanols and *n*-alkanes increased throughout the entire soil profiles in the grassy matrix; in contrast, these concentrations decreased and then increased in the shrub patches (Table 2). The concentrations of the free lipid groups were significantly higher in the shrub patches than those in the grassy matrix, but only in the top 0–30 cm ( $p < 0.05$ ; Table 2). Specifically, the concentrations of the major base hydrolysis products sharply increased between 70 and 100 cm in both the grass matrix and shrub patches, and their abundance was much higher in the grassy matrix (Table 2). Moreover, the lignin-derived phenols were most abundant, followed by bound lipids and then free lipids in both the grass matrix and the shrub patches (Table 3). The concentration of lignin-derived phenols decreased at first but then increased with depth in both the shrub patches and the grassy matrix (Table 2). In the upper 50 cm, the lignin concentration was much more abundant in the shrub patches (10.84–14.93 mg/g OC) than in the grassy matrix (7.09–9.24 mg/g OC) ( $p = 0.08$  and 0.06).

### PCA for SOM composition at different soil depths

The PCA was conducted based on multiple biomarkers to assess the vertical distribution of SOM composition and degradation in the shrub patches and the grassy matrix. The PCs explained 60% of the variation (Fig. 4). Free lipid, bound lipid and lignin contents had strong loadings along PC1, while the C/V and  $(\text{Ad}/\text{Al})_s$  ratios had strong loadings along PC2. Based on these components and parameters, the samples in the shrub patches and the grassy matrix could be separated by PC2. In addition, their vertical patterns were quite different. For example, the PC scores of the grassy matrix samples increased throughout the entire soil profile; however, in the shrub patches, the scores decreased along PC1 in the upper 50 cm and then increased below 50 cm. Moreover, the range in variation was smaller in the shrub patch.

**Fig. 3** The vertical distribution of products from solvent extraction, including *n*-alkanoic acids (FAs), *n*-alkanols, and *n*-alkanes, and base hydrolysis, including bound *n*-FAs,  $\alpha,\omega$ -alkanedioic acids (DAs),  $\omega$ -hydroxyalkanoic acids (OH FAs) and *a*-OH FAs in the grassy matrix and the shrub patch ( $n = 9$  in each layer and at each sampling position). The concentrations of all biomarkers were standardized to mg/g OC



## Discussion

Shrub encroachment in grasslands has been shown to alter the carbon balance and dynamics (Eldridge et al. 2011; Li et al. 2016). Using a molecular biomarker approach, we found that both the carbon content and the chemical compositions of grassland soils were influenced by shrub encroachment (Table 2). To the best of our knowledge, this study represents the first assessment of the vertical distribution patterns of molecular-level SOC composition following shrub encroachment. Zhou et al. (2017b) found that root density in the shrub patches was higher than that in the grassy matrix along a 1.2-m soil profile, strongly suggesting the potential of carbon sequestration in the subsoil with shrub encroachment.

### Vertical variability in SOM reflected by specific biomarkers and parameters

The dominant  $C_{18}$  *n*-FAs, long-chain *n*-alkanols and  $C_{29}$ ,  $C_{31}$  *n*-alkanes, which are specific biomarkers in local plant leaves, increased with soil depth, especially in the grassy matrix. These results suggest a great contribution of plants, particularly the aboveground inputs, and that the translocation of leaf-derived carbon into the subsoil is an important process (Zhou et al. 2017a). Consistent with previous studies, higher concentrations of free lipids in the shrub patches were observed only in the 0–30 cm layers, indicating that aboveground inputs greatly contribute to SOC in the topsoil (Filley et al. 2008; Tamura and Tharayil 2014). This inference was

**Table 2** Biomarker and parameter distributions in the grassy matrix and the shrub patch

Item	Grassy matrix				Shrub patch			
	0–30 cm	30–50 cm	50–70 cm	70–100 cm	0–30 cm	30–50 cm	50–70 cm	70–100 cm
Compound name								
Soil physical properties								
SOC (%)	0.43 ± 0.03A	0.34 ± 0.05A	0.21 ± 0.04B	0.16 ± 0.05B	0.32 ± 0.05	0.29 ± 0.04	0.27 ± 0.03	0.21 ± 0.03
STN (%)	0.05 ± 0.00A	0.04 ± 0.00AB	0.03 ± 0.00 BC	0.02 ± 0.00C	0.04 ± 0.00	0.04 ± 0.00	0.04 ± 0.01	0.03 ± 0.00
STP (%)	0.21 ± 0.01	0.19 ± 0.01	0.17 ± 0.01	0.17 ± 0.02	0.17 ± 0.01	0.16 ± 0.01	0.15 ± 0.01	0.15 ± 0.01
pH	8.90 ± 0.07A	9.17 ± 0.06B	9.34 ± 0.03 <sup>BC</sup>	9.4 ± 0.06 <sup>C</sup>	9.05 ± 0.08	9.12 ± 0.04	9.11 ± 0.07 <sup>*</sup>	9.16 ± 0.11 <sup>*</sup>
Solvent-extractable compounds (mg g <sup>-1</sup> OC)								
<i>n</i> -alkanoic acids	1.26 ± 0.24 <sup>*</sup>	1.56 ± 0.29	1.44 ± 0.44	2.55 ± 0.81	2.24 ± 0.30 <sup>*</sup>	1.96 ± 0.20	1.61 ± 0.30	1.79 ± 0.29
<i>n</i> -alkanols	0.47 ± 0.09 <sup>*</sup>	0.54 ± 0.14	0.92 ± 0.35	1.17 ± 0.51	0.80 ± 0.11 <sup>*</sup>	0.65 ± 0.10	1.13 ± 0.26	0.78 ± 0.18
<i>n</i> -alkanes	0.19 ± 0.04 <sup>*</sup>	0.20 ± 0.06	0.23 ± 0.07	0.31 ± 0.10	0.41 ± 0.06 <sup>*</sup>	0.26 ± 0.04	0.24 ± 0.04	0.29 ± 0.07
Ergosterol	0.01 ± 0.00 <sup>*</sup>	0.01 ± 0.00	0.01 ± 0.00	0.01 ± 0.00	0.04 ± 0.01 <sup>a</sup>	0.02 ± 0.00b	0.02 ± 0.00b	0.02 ± 0.01b
Hydrolysable lipids (mg g <sup>-1</sup> OC)								
$\alpha$ -hydroxyalkanoic acids	0.02 ± 0.01	nd	0.06 ± 0.02	0.18 ± 0.08	0.02 ± 0.01a	0.02 ± 0.01a	0.03 ± 0.02a	0.06 ± 0.04b
$\omega$ -hydroxyalkanoic acids	0.78 ± 0.18	0.61 ± 0.14	0.69 ± 0.15	3.67 ± 1.69	1.15 ± 0.14a	0.60 ± 0.14a	0.75 ± 0.15a	1.96 ± 0.67b
$\alpha,\omega$ -alkanedioic acids	0.48 ± 0.06	0.75 ± 0.19	0.63 ± 0.24	2.21 ± 0.59	0.91 ± 0.23	0.65 ± 0.22	0.48 ± 0.17	0.95 ± 0.22
<i>n</i> -alkanoic acids	1.38 ± 0.27	1.89 ± 0.36	2.51 ± 1.09	8.56 ± 2.64	2.63 ± 0.57	1.89 ± 0.44	1.70 ± 0.47	3.50 ± 0.92
Both in cutin and suberin	0.48 ± 0.09	0.80 ± 0.24	0.70 ± 0.38	3.47 ± 1.41	0.73 ± 0.13a	0.39 ± 0.09a	0.43 ± 0.08a	1.57 ± 0.60b
Suberin	0.78 ± 0.18	0.56 ± 0.12 <sup>*</sup>	0.62 ± 0.21	3.54 ± 1.44	1.34 ± 0.17 <sup>a</sup>	0.86 ± 0.19a	0.80 ± 0.26a	1.33 ± 0.35b
Lignin-derived phenols (mg g <sup>-1</sup> OC)								
Lignin	9.24 ± 2.10A	7.09 ± 1.43AB	8.94 ± 1.72B	10.48 ± 2.28B	14.93 ± 1.77	10.84 ± 1.61	8.14 ± 1.45	10.01 ± 2.01
Cinnamyls	1.71 ± 0.39	1.37 ± 0.23	1.87 ± 0.30	2.23 ± 0.48	2.34 ± 0.26	1.84 ± 0.23	1.38 ± 0.21	1.74 ± 0.30
Syringyls	3.23 ± 0.79 <sup>A</sup>	2.34 ± 0.48 <sup>AB</sup>	2.97 ± 0.58B	3.41 ± 0.78B	5.58 ± 0.72 <sup>*</sup>	3.85 ± 0.53 <sup>*</sup>	2.84 ± 0.52	3.53 ± 0.73
Vanillyls	4.30 ± 0.93 <sup>*</sup>	3.39 ± 0.73	4.10 ± 0.87	4.85 ± 1.09	7.01 ± 0.83 <sup>*</sup>	5.16 ± 0.88	3.92 ± 0.72	4.74 ± 0.99
V: S: C	2.51:1.89:1	2.47:1.71:1	2.19:1.59:1	2.17:1.53:1	3.00:2.38:1	2.80:2.09:1	2.84:2.06:1	2.72:2.03:1
Parameters								
P <sub>mtl</sub>	1.08 ± 0.15	1.18 ± 0.22	1.35 ± 0.15	1.22 ± 0.22	0.98 ± 0.15	1.21 ± 0.19	1.24 ± 0.13	1.60 ± 0.31
C <sub>27</sub> /C <sub>31</sub> <i>n</i> -alkanes	0.39 ± 0.07 <sup>*</sup>	0.70 ± 0.15	0.98 ± 0.20 <sup>*</sup>	1.15 ± 0.25	0.22 ± 0.02 <sup>*</sup>	0.42 ± 0.05	0.53 ± 0.06 <sup>*</sup>	0.62 ± 0.11
$\omega$ -C <sub>16</sub> / $\Sigma$ C <sub>16</sub>	0.30 ± 0.01	0.23 ± 0.03	0.29 ± 0.04	0.27 ± 0.04	0.28 ± 0.01	0.22 ± 0.05	0.29 ± 0.01	0.31 ± 0.02
Suberin/Cutin	3.13 ± 0.72	2.22 ± 0.38 <sup>*</sup>	3.43 ± 0.94	1.70 ± 0.21	3.24 ± 0.37	3.75 ± 0.79 <sup>*</sup>	3.56 ± 0.75	2.03 ± 0.31
C/N	0.39 ± 0.01 <sup>*</sup>	0.50 ± 0.09	0.55 ± 0.08 <sup>*</sup>	0.54 ± 0.10	0.34 ± 0.01 <sup>*</sup>	0.39 ± 0.05	0.36 ± 0.01 <sup>*</sup>	0.43 ± 0.04
S/V	0.73 ± 0.05	0.75 ± 0.05	0.76 ± 0.04	0.73 ± 0.06	0.80 ± 0.03	0.77 ± 0.03	0.72 ± 0.02	0.75 ± 0.03
(Ad/Al) <sub>s</sub>	0.62 ± 0.02	0.69 ± 0.06	0.74 ± 0.08	0.73 ± 0.09	0.63 ± 0.05	0.63 ± 0.03	0.63 ± 0.04	0.68 ± 0.07
(Ad/Al) <sub>v</sub>	0.71 ± 0.06	0.83 ± 0.06	0.87 ± 0.09	0.90 ± 0.08	0.83 ± 0.11	0.80 ± 0.04	0.85 ± 0.06	0.84 ± 0.05

<sup>a</sup> \*Significant differences ( $p < 0.05$ ) in the shrub patch and the grassy matrix in the same layer

<sup>b</sup> Significant differences ( $p < 0.05$ ) in different soil depths are indicated by capital and lower-case letters for the grassy matrix and the shrub patch, respectively

<sup>c</sup> P<sub>mtl</sub> =  $\sum_{FA}(C_{14} - C_{18}) / \sum_{FA}(C_{20})$  (Angst et al. 2016)



**Table 3** The relative proportion of lignin, free lipids and bound lipids at different soil depths

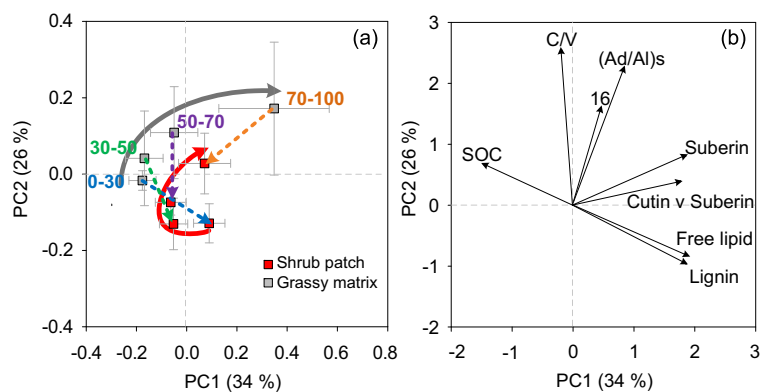
Sampling position	Mean $\pm$ standard error (%)			Range (%)			
	Depth	Lignin	Free lipid	Bound lipid	Lignin	Free lipid	Bound lipid
Grassy matrix	0–30	61.5 $\pm$ 4.5	15.5 $\pm$ 1.7	23.0 $\pm$ 3.3	34.6–80.8	6.8–24.5	8.8–40.9
	30–50	51.9 $\pm$ 4.8	16.9 $\pm$ 1.7	31.2 $\pm$ 6.3	34.1–71.9	8.8–26.6	6.2–54.2
	50–70	60.9 $\pm$ 3.8	16.6 $\pm$ 2.6	22.5 $\pm$ 5.7	33.1–73.0	0.7–26.7	10.3–66.2
	70–100	40.8 $\pm$ 4.1	12.7 $\pm$ 2.4	46.5 $\pm$ 5.1	28.6–64.0	0.9–21.7	14.4–61.1
Shrub patch	0–30	64.3 $\pm$ 3.3	14.8 $\pm$ 0.8	20.9 $\pm$ 3.1	44.5–73.9	10.4–17.8	8.3–37.8
	30–50	63.6 $\pm$ 3.4	17.3 $\pm$ 0.9	19.1 $\pm$ 4.0	49.3–76.9	12.4–20.4	4.3–38.3
	50–70	57.9 $\pm$ 2.0	20.8 $\pm$ 2.7	21.4 $\pm$ 2.6	45.3–65.5	5.1–31.7	10.2–36.3
	70–100	51.7 $\pm$ 4.7	16.3 $\pm$ 2.5	32.1 $\pm$ 3.6	31.3–76.4	2.3–29.0	21.3–48.2
Total	0–30	62.9 $\pm$ 2.7	15.2 $\pm$ 0.9	21.9 $\pm$ 2.2	34.6–80.8	6.8–24.5	8.3–40.9
	30–50	57.8 $\pm$ 3.2	17.1 $\pm$ 0.9	25.2 $\pm$ 3.9	34.1–76.9	8.8–26.6	4.3–54.2
	50–70	59.4 $\pm$ 2.1	18.8 $\pm$ 1.9	22.0 $\pm$ 3.0	33.1–73.0	0.7–31.7	10.2–66.2
	70–100	46.3 $\pm$ 3.3	14.4 $\pm$ 1.7	39.3 $\pm$ 3.5	28.6–76.4	0.9–29.0	14.4–61.1

further confirmed by the low  $P_{\text{rml}}$  value, and the abundant concentrations of  $C_{29}$  and  $C_{31}$  *n*-alkanes in the topsoil of the shrub patches (Table 2; Angst et al. 2016; Zhou et al. 2017a). Consistent with previous studies, ergosterol, a valuable biomarker for fungi, was identified in higher abundances only in the upper 30 cm of the soils, which suggests higher fungal activities in the topsoil (Feng and Simpson 2007; Feng et al. 2010). Similarly,  $C_{29}$  *n*-alkane, which is an indicator of local shrub leaves, was abundant in the shrub patches, suggesting the great contribution of shrub leaves to the topsoil OC (Fig. 3; Zhou et al. 2017a).

$C_{27}$  *n*-alkanes, which are detected only in the roots of local plants, increased with soil depth in both the shrub patches and the grassy matrix, suggesting increased belowground inputs to SOC (Jobbágy and Jackson

2000; Zhou et al. 2017a). In addition, suberin was detected at low abundances in the upper 70 cm, but increased sharply between 70 and 100 cm, reflecting enhanced root inputs and the eluviation process, which translocates surface SOM into deeper soil layers and dilutes the suberin concentrations (Feng and Simpson 2007). This translocation process is more important in our soils with a sandy texture (sand content of approximately 80–90%; Wu et al. 2016) or high permeability (Rumpel and Kögel-Knabner 2011; Zhao et al. 2014; Angst et al. 2016). The sharp accumulation in 70–100 cm might also be partly linked to the abundant clay and silt content. Clay and silt sized minerals play an important role in providing protection for SOC composition due to their high specific surface area and hydroxylated reactive surfaces (Doetterl et al. 2015; Han et al.

**Fig. 4** Principal component analysis (PCA) based on the SOC composition and parameters. **a** Scores of samples in the shrub patch and the grassy matrix (mean  $\pm$  standard error,  $n = 9$ ); **b** Scores of biomarkers and parameters. Dotted arrows are vectors where the grassy matrix pointed to the shrub patches in the same layer



2016). Moreover, the long-chain *n*-alkanes were recalcitrant soil fractions and have been used as indicators for past vegetation in geological studies (Andersson et al. 2011; Angst et al. 2016). The slight increase in the abundance of *n*-alkanes with soil depth also suggests that some of the SOC in the subsoil can be inherited from parent materials (Fig. 3, Otto and Simpson 2005; Nguyen Tu et al. 2011; Angst et al. 2016).

The concentration of lignin-derived phenols decreased in the upper 50 cm depth, mostly due to the decrease in litter inputs with soil depth (Feng and Simpson 2007). Cinnamyls are biomarkers of non-woody tissues (Lam et al. 2001) and are more labile than syringyls and vanillyls (Hedges et al. 1988). The higher C/V ratio in the deep soils of both the grass matrix and the shrub patch was surprising (Table 2). Because C/V and S/V ratios are higher in leaves than in roots (Zhou et al. 2017a), such a depth-distribution pattern reflects the eluviation of aboveground carbon from herb or shrub litters (Table 2; Otto and Simpson 2006). Cinnamyls can translocate quickly into the subsoil, where lower fungal activities (reflected by lower concentrations of ergosterol) provide favorable conditions for their preservation; they would otherwise be preferentially degraded in the topsoil (Table 2; Feng et al. 2010). Compared to the grassy matrix, the shrub patches had higher C/V values, reflecting the lower proportion of non-woody carbon inputs as a result of shrub encroachment in the grassland (Zhou et al. 2017a).

#### Changes in the chemical composition of SOM following shrub encroachment

The PCA based on the SOC biomarkers and parameters showed that these compounds had strong loadings on PC1, while the C/V and (Ad/Al)<sub>s</sub> ratios had strong loadings on PC2 (Fig. 4), indicating that PC1 represents the chemical composition of the OM, while PC2 represents the degradation status of lignin. The SOC composition of the shrub patches varied along PC1 in the upper 50 cm and along PC2 below 50 cm, suggesting changes in the origin of inputs along the entire 1-m profile and the enhanced degradation of lignin in 50–100 cm layer (Fig. 4). The SOC of the shrub patches was mainly derived from leaves in the upper layer and from roots in the deeper layers (Zhou et al. 2017a), as confirmed by the varying relationship between the C/V ratio and the S/V ratio (indicators of lignin origin; Fig. 6; Otto and

Simpson 2006; Zhou et al. 2017a). Furthermore, in the shrub patches, the SOC composition was more relevant to input chemistry in 0–50 cm, but was more relevant to degradation in the 50–100 cm layer (Fig. 4). In comparison, the SOC composition of the grassy matrix varied regularly along the PCs (Fig. 4), indicating regular root inputs and enhanced lignin degradation (Bao et al. 2017). This result was further confirmed by the stable relationship between the C/V ratio and the S/V ratio (Fig. 6) and the varying direction of SOC composition toward to the suberin biomarker in the PCA results (Fig. 4; Angst et al. 2016; Zhou et al. 2017a).

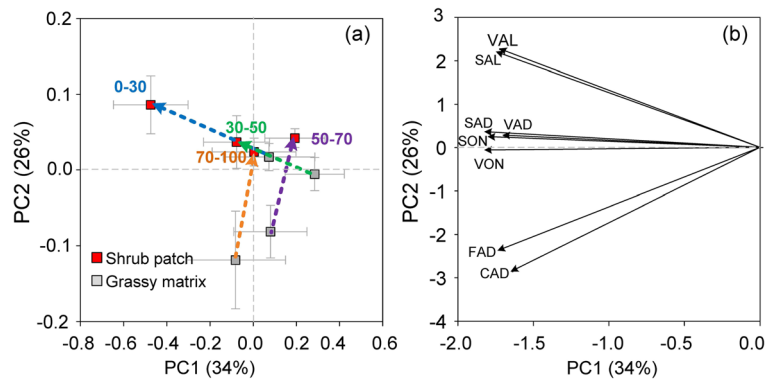
In addition, the chemical composition of the largest contributor, lignin-derived phenols, varied along PC1 in the shrub patches but along PC2 in the grassy matrix, suggesting different source (Fig. 5) and degradation characteristics (Fig. 6; Bao et al. 2017). The ratios of Ad/Al (degradation indicators of lignin) were much higher in the soil than those in the fresh plants (Zhou et al. 2017a), indicating that the lignin in the soil had been significantly oxidized. It has long been noted that lignin is mainly degraded by white-rot and brown-rot fungi, and the presence of fungi in the topsoil is confirmed by ergosterol, the greater abundance of which might be the reason for the greater oxidation of lignin. (Table 2; Feng et al. 2010; Zhao et al. 2014). In addition, the positive correlation between the (Ad/Al)<sub>v</sub> and (Ad/Al)<sub>s</sub> ratios showed the simultaneous oxidation of vanillyls and syringyls phenols in the grassy matrix, which was not observed in the shrub patches (Fig. 6; Otto and Simpson 2006; Bao et al. 2017).

#### Implications for SOC composition changes along the soil profile following shrub encroachment

The C<sub>27</sub>–C<sub>31</sub> *n*-alkanes, C<sub>16</sub>–C<sub>32</sub> *n*-FAs and long-chain *n*-alkanols isolated using solvent extractions are indicators of plant waxes (Nierop 1998; Zhou et al. 2017a). The C<sub>18</sub> bound *n*-FAs and C<sub>16</sub> DAs in bound lipids are derived from leaves, and the C<sub>20</sub> ω-OH FAs are derived from the roots (Otto and Simpson 2005, 2006; Zhou et al. 2017a). Our results emphasize the importance of plant inputs for SOC stocks in the SEGs when compared to microbial-derived carbon. Our results also have important implications for the vertical distribution of carbon after shrub encroachment.

Previous studies have proposed that the chemistry and quantity of plant inputs directly influence the SOM composition, and the relationships vary in

**Fig. 5** Principal component analyses (PCA) based on lignin-derived phenols. **a** Scores of samples in the shrub patch and grassy matrix (mean  $\pm$  standard error,  $n = 9$ ); **b** Scores of biomarkers and parameters

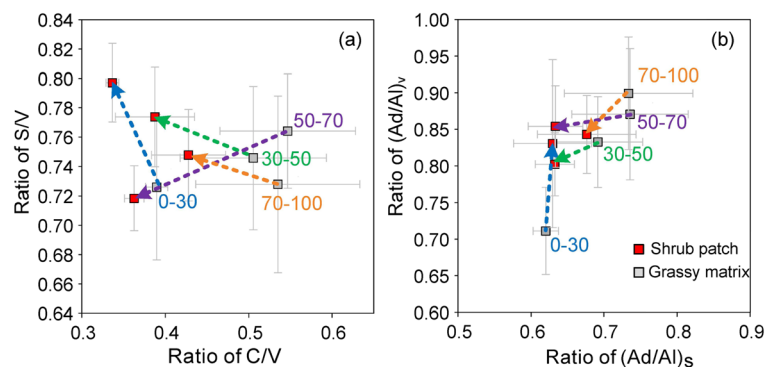


different ecosystems (Pisani et al. 2016; Kögel-Knabner 2017). In our present study, the vertical distribution patterns of the compounds and parameters (i.e., *n*-alkanols, *n*-alkanes, ergosterol,  $\omega$ -OH FAs and syringyls) were similar to those in the Alberta grasslands (Feng and Simpson 2007). Steffens et al. (2011) found that particulate OM decomposition did not change with depth in a grazed Inner Mongolian steppe using solid-state  $^{13}\text{C}$  NMR spectroscopy, which was in contrast to lignin degradation in our SEG sites (Figs. 4 and 6b). Surprisingly, the  $P_{\text{mnl}}$  ratio and the *n*-FAs, *n*-alkanes and suberin contents showed similar vertical patterns to those of European beech forests (Angst et al. 2016). These comparisons indicated that shrub encroachment changed the SOC composition and degradation state of the grasslands.

The vanillyls to syringyls to cinnamyls (V: S: C) ratio was approximately 3:2:1 along the entire 1-m profile in the shrub patches (Table 2). Similarly, the soils in the grassy matrix were characterized by a V: S: C ratio of 3:2:1 in the upper 30 cm and a ratio of 2:2:1 below 30 cm. This ratio differs from previously reported values for grassland soils or non-woody

sources (i.e., 1:1:1; Otto et al. 2005; Feng and Simpson 2007; Zhou et al. 2017a); however, our previous results showed similar characteristics in *C. microphylla* tissues (i.e., 3:2:1; Zhou et al. 2017a). In addition, the vertical similarities between the biomarkers of the grassy matrix and the shrub patches (Table 2) demonstrated that shrub encroachment influenced the soil C composition under the shrub canopy as well as in the grassy matrix (Maestre et al. 2009). Similarly, Peterson and Neill (2003) revealed that soil carbon patterns changed rapidly and closely resembled permanent grassland after only 2 years of transition from forest to grassland. These changes could be explained by the architectural and physiological differences between the root systems of sprouting shrubs and herbs (Maestre et al. 2009). Herbs, such as *Stipa*, create near-surface and limited roots under the canopy (Maestre et al. 2009); in contrast, the roots of *C. microphylla* can extend several meters horizontally and 1.8 m vertically (Xiong and Han 2005; Niu et al. 2013; Zhou et al. 2017a). Consequently, shrub encroachment could influence SOC stocks by changing root distribution

**Fig. 6** Lignin source parameter (a) and degradation parameter (b) changes with soil depth in the shrub patch and the grassy matrix.  $n = 9$  for each parameter and depth increment. (Ad/Al)<sub>v</sub>, vanillic acid/vanillin ratio; (Ad/Al)<sub>s</sub>, syringic acid/syringaldehyde ratio



patterns. The horizontal distance over which shrub encroachment can influence SOC needs further study.

## Conclusions

Based on a SOM biomarker approach, our study provides the first assessment of the vertical patterns in molecular-level C composition after shrub encroachment. The SOC composition in the shrub patches were negatively related to the free lipid, cutin, suberin and lignin compounds in the upper 50 cm layer. In comparison, the SOC composition was positively related to the (Al/Ad)<sub>s</sub> ratio and suberin contents along the entire 1-m profile in the grassy matrix and the 50–100 cm layer in the shrub patches. On the other hand, the vanillyls to syringyls to cinnamyls ratio was approximately 3:2:1 in the shrub patches and 3:2:1 or 2:2:1 in the grassy matrix. This study shows that shrub encroachment and soil processes (such as percolation) strongly affected the vertical distribution of SOC composition. Our results also highlight the different vertical patterns of SOC composition between the shrub patches and the grassy matrix in the upper 50 cm layer. Moreover, the similarity of lignin composition between shrub patches and grassy matrix suggests that shrub encroachment influenced the SOC composition not only under the shrub canopy but also in the grassy matrix via the horizontal extension of the root systems of the sprouting shrubs. Our results provided new insights into the vertical patterns of SOC changes after shrub encroachment at the molecular level, and have important implications for understanding the mechanisms of soil carbon dynamics with changes in vegetation structure and composition.

**Acknowledgements** This study was funded by the National Natural Science Foundation of China (31330012, 31470525), the National Basic Research Program of China on Global Change (2014CB954001), the Key Research Program of Frontier Sciences, CAS, (QYZDY-SSW-SMC011).

## References

- Andersson RA, Kuhry P, Meyers P, Zebühr Y (2011) Impacts of paleohydrological changes on *n*-alkane biomarker compositions of a holocene peat sequence in the eastern European Russian Arctic. *Org Geochem* 42:1065–1075
- Angst G, John S, Mueller CW, Kögel-Knabner I, Rethemeyer J (2016) Tracing the sources and spatial distribution of organic carbon in subsoils. *Sci Rep* 6. <https://doi.org/10.1038/srep28974>
- Armas-Herrera CM, Dignac M, Rumpel C, Arbelo AD, Chabbi A (2016) Management effects on composition and dynamics of cutin and suberin in topsoil under agricultural use. *Eur J Soil Sci* 67:360–373
- Bao H, Kao S, Lee T, Zehetner F, Huang J, Chang Y, Lu J, Lee J (2017) Distribution of organic carbon and lignin in soils in a subtropical small mountainous river basin. *Geoderma* 306: 81–88
- Blaser WJ, Shanungu GK, Edwards PJ, Olde Venterink H (2014) Woody encroachment reduces nutrient limitation and promotes soil carbon sequestration. *Ecol Evol* 4:1423–1438
- Briske DD (2017) Rangeland systems: processes, management and challenges. Springer. <https://doi.org/10.1007/978-3-319-46709-2>
- Bull ID, Nott CJ, van Bergen PF, Poulton PR, Evershed RP (2000) Organic geochemical studies of soils from the rothamsted classical experiments-VI. The occurrence of organic acids in an experimental grassland soil. *Soil Biol Biochem* 32:1367–1376
- Cai Y, Tang Z, Xiong G, Xie Z, Liu Z, Feng X (2017) Different composition and distribution patterns of mineral-protected versus hydrolysable lipids in shrubland soils. *J Geophys Res Biogeosci* 122:2206–2218
- Chen L, Li H, Zhang P, Zhao X, Zhou L, Liu T, Hu H, Bai Y, Shen H, Fang J (2015) Climate and native grassland vegetation as drivers of the community structures of shrub-encroached grasslands in Inner Mongolia, China. *Landsc Ecol* 30: 1627–1641
- Crow SE, Lajtha K, Filley TR, Swanston CW, Bowden RD, Caldwell BA (2009) Sources of plant-derived carbon and stability of organic matter in soil: implications for global change. *Glob Chang Biol* 15:2003–2019
- Doetterl S, Stevens A, Six J, Merckx R, Oost KV, Pinto MC, Casanova-Katny A, Muñoz C, Boudin M, Venegas EZ, Boeckx P (2015) Soil carbon storage controlled by interactions between geochemistry and climate. *Nat Geosci* 8:780–783
- Eldridge DJ, Bowker MA, Maestre FT, Roger E, Reynolds JF, Whitford WG (2011) Impacts of shrub encroachment on ecosystem structure and functioning: towards a global synthesis. *Ecol Lett* 14:709–722
- Feng X, Simpson MJ (2007) The distribution and degradation of biomarkers in Alberta grassland soil profiles. *Org Geochem* 38:1558–1570
- Feng X, Simpson MJ (2011) Molecular-level methods for monitoring soil organic matter responses to global climate change. *J Environ Monit* 13:1246–1254
- Feng X, Simpson AJ, Schlesinger WH, Simpson MJ (2010) Altered microbial community structure and organic matter composition under elevated CO<sub>2</sub> and N fertilization in the Duke forest. *Glob Chang Biol* 16:2104–2116
- Filley TR, Boutton TW, Liao JD, Jastrow JD, Gamblin DE (2008) Chemical changes to nonaggregated particulate soil organic matter following grassland-to-woodland transition in a subtropical savanna. *J Geophys Res* 113:G03009
- Han L, Sun K, Jin J, Xing B (2016) Some concepts of soil organic carbon characteristics and mineral interaction from a review of literature. *Soil Biol Biochem* 94:107–121

- Hedges JI, Mann DC (1979) The characterization of plant tissues by their lignin oxidation products. *Geochim Cosmochim Acta* 43:1803–1807
- Hedges JI, Blanchette RA, Weliky K, Devol AH (1988) Effects of fungal degradation on the CuO oxidation products of lignin: a controlled laboratory study. *Geochim Cosmochim Acta* 52:2717–2726
- Hughes RF, Archer SR, Asner GP, Wessman CA, McMurtry C, Nelson JIM, Ansley RJ (2006) Changes in aboveground primary production and carbon and nitrogen pools accompanying woody plant encroachment in a temperate savanna. *Glob Chang Biol* 12:1733–1747
- IUSS Working Group WRB (2015) World reference base for soil resources 2014, update 2015 international soil classification system for naming soils and creating legends for soil maps. World Soil resources Reports No. 106. FAO, Rome
- Jackson RB, Banner JL, Jobbágy EG, Pockman WT, Wall DH (2002) Ecosystem carbon loss with woody plant invasion of grasslands. *Nature* 418:623–626
- Jobbágy EG, Jackson RB (2000) The vertical distribution of soil organic carbon and its relation to climate and vegetation. *Ecol Appl* 10:423–436
- Knapp AK, Briggs JM, Collins SL, Archer SR, Bret-Harte MS, Ewers BE, Peters DP, Young DR, Shaver GR, Pendall E, Cleary MB (2008) Shrub encroachment in north American grasslands: shifts in growth form dominance rapidly alters control of ecosystem carbon inputs. *Glob Chang Biol* 14:615–623
- Kögel-Knabner I (2002) The macromolecular organic composition of plant and microbial residues as inputs to soil organic matter. *Soil Biol Biochem* 34:139–162
- Kögel-Knabner I (2017) The macromolecular organic composition of plant and microbial residues as inputs to soil organic matter: fourteen years on. *Soil Biol Biochem* 105:A3–A8
- Lam TBT, Kadoya K, Iiyama K (2001) Bonding of hydroxycinnamic acids to lignin: Ferulic and *p*-coumaric acids are predominantly linked at the benzyl position of lignin, not the  $\beta$ -position, in grass cell walls. *Phytochemistry* 57:987–992
- Li H (2015) Effects of shrub encroachment on soil organic carbon pool in Inner-Mongolia, China. PhD thesis, Institute of Botany, Chinese Academy of Sciences, Beijing
- Li H, Shen H, Chen L, Liu T, Hu H, Zhao X, Zhou L, Zhang P, Fang J (2016) Effects of shrub encroachment on soil organic carbon in global grasslands. *Sci Rep* 6:28974
- Maestre FT, Bowker MA, Puche MD, Belén Hinojosa M, Martínez I, García-Palacios P, Castillo AP, Soliveres S, Luzuriaga AL, Sánchez AM (2009) Shrub encroachment can reverse desertification in semi-arid Mediterranean grasslands. *Ecol Lett* 12:930–941
- National soil survey office (1994) A database of soil types in China. China Agriculture Press, Beijing
- Nguyen Tu TT, Egasse C, Zeller B, Bardoux G, Biron P, Ponge J, David B, Derenne S (2011) Early degradation of plant alkanes in soils: a litterbag experiment using C-13-labelled leaves. *Soil Biol Biochem* 43:2222–2228
- Nierop KGJ (1998) Origin of aliphatic compounds in a forest soil. *Org Geochem* 29:1009–1016
- Nierop KGJ, Naafs DFW, Verstraten JM (2003) Occurrence and distribution of ester-bound lipids in dutch coastal dune soils along a pH gradient. *Org Geochem* 34:719–729
- Niu C, Alamusa ZQ, Luo Y, Toshio O, Sun G, Liu Q (2013) Allocation patterns of above- and below-ground biomass of *Caragana microphylla* in Horqin Sandy land, North China. *China J Eco* 32:1980–1986
- Oelofse M, Birch-Thomsen T, Magid J, de Neergaard A, van Deventer R, Bruun S, Hill T (2016) The impact of black wattle encroachment of indigenous grasslands on soil carbon, eastern Sape, South Africa. *Biol Invasions* 18:445–456
- Otto A, Simpson MJ (2005) Degradation and preservation of vascular plant-derived biomarkers in grassland and forest soils from Western Canada. *Biogeochemistry* 74:377–409
- Otto A, Simpson MJ (2006) Evaluation of CuO oxidation parameters for determining the source and stage of lignin degradation in soil. *Biogeochemistry* 80:121–142
- Otto A, Shunthirasingham C, Simpson MJ (2005) A comparison of plant and microbial biomarkers in grassland soils from the prairie ecozone of Canada. *Org Geochem* 36:425–448
- Peng H, Li X, Jiang Z, Ma Y, Li G, Zhang Z, Zhang S, Li L, Zhao G (2013) Shrub encroachment with increasing anthropogenic disturbance in the semiarid Inner Mongolian grasslands of China. *Catena* 109:39–48
- Peterson GG, Neill C (2003) Using soil  $^{13}\text{C}$  to detect the historic presence of *Schizachyrium scoparium* (little bluestem) grasslands on Martha's vineyard. *Restor Ecol* 11:116–122
- Pisani O, Frey SD, Simpson AJ, Simpson MJ (2015) Soil warming and nitrogen deposition alter soil organic matter composition at the molecular-level. *Biogeochemistry* 123:391–409
- Pisani O, Haddix ML, Conant RT, Paul EA, Simpson MJ (2016) Molecular composition of soil organic matter with land-use change along a bi-continental mean annual temperature gradient. *Sci Total Environ* 573:470–480
- Rumpel C, Eusterhues K, Kögel-Knabner I (2004) Location and chemical composition of stabilized organic carbon in topsoil and subsoil horizons of two acid forest soils. *Soil Biol Biochem* 36:177–190
- Rumpel C, Kögel-Knabner I (2011) Deep soil organic matter—a key but poorly understood component of terrestrial C cycle. *Plant Soil* 338:143–158
- Saixiyala, Yang D, Zhang S, Liu G, Yang X, Huang Z, Ye X (2017) Facilitation by a spiny shrub on a rhizomatous clonal herbaceous in thickening-grassland in northern China: Increased soil resources or shelter from herbivores. *Front Plant Sci* 8:809
- Salomé C, Nunan N, Pouteau V, Lerch TZ, Chenu C (2010) Carbon dynamics in topsoil and in subsoil may be controlled by different regulatory mechanisms. *Glob Chang Biol* 16:416–426
- Schmidt MW, Tom MS, Abiven S, Dittmar T, Guggenberger G, Janssens IA, Kleber M, Kögel-Knabner I, Lehmann J, Manning DA, Nannipieri P, Rasse DP, Weiner S, Trumbore SE (2011) Persistence of soil organic matter as an ecosystem property. *Nature* 478:49–56
- Steffens M, Kölbl A, Schörk E, Gschrey B, Kögel-Knabner I (2011) Distribution of soil organic matter between fractions and aggregate size classes in grazed semiarid steppe soil profiles. *Plant Soil* 338:63–81
- Tamura M, Tharayil N (2014) Plant litter chemistry and microbial priming regulate the accrual, composition and stability of soil carbon in invaded ecosystems. *New Phytol* 203:110–124
- Toriyama J, Kato T, Siregar CA, Siringoringo HH, Ohta S, Kiyono Y (2011) Comparison of depth- and mass-based approaches



- for estimating changes in forest soil carbon stocks: a case study in young plantations and secondary forests in west Java, Indonesia. *Forest Ecol Manag* 262:1659–1667
- Van Auken OW (2009) Causes and consequences of woody plant encroachment into Western North American grasslands. *J Environ Manag* 90:2931–2942
- Wang J, Guo Y, Yao Y, Tang J, Zhang M (2017) Distribution characteristics of root system and carbon stock of *Caragana microphylla* Lam, in Aohan sandifunctional area. *Nat Sci Ed* 45:103–110
- Wu M, Zhang Y, Song Y, Zhao B (2016) Study on soil texture of typical steppes in Central Inner Mongolia. *Environ Dev* 28:12–15
- Xiong X, Han X (2005) Spatial heterogeneity in soil carbon and nitrogen resources, caused by *Caragana microphylla*, in the thickening of semiarid grassland, Inner Mongolia. *Acta Ecologica Sinica* 25:1678–1683
- Zhang L, Wang X, Zhang W, Hu E, Hai L (2013) Study on population structure and spatial distribution characteristic of *Amygdalus pedunculata* in two habitats. *J Arid Land Resour Environ* 27:124–129
- Zhao L, Wu W, Xu X, Xu Y (2014) Soil organic matter dynamics under different land use in grasslands in Inner Mongolia (northern China). *Biogeosciences* 11:5103–5113
- Zhou L, Li H, Shen H, Xu Y, Wang Y, Xing A, Fang J (2017a) Shrub-encroachment induced alterations in input chemistry and soil microbial community affect topsoil organic carbon in an inner Mongolian grassland. *Biogeochemistry* 136:311–324
- Zhou Y, Boutton TW, Wu XB, McCulley R (2017b) Soil carbon response to woody plant encroachment: importance of spatial heterogeneity and deep soil storage. *J Ecology* 105:1738–1749